 DOI: 10.5281/zenodo.14269036

Characterisation of the biocompatible $Ti_{60}Zr_{10}Nb_{15}Si_{15}$ powder for metallic glass produced by selective laser melting

M. Li[1*], H. Mozaffari-Jovein[1]

[1] Institute of Materials Science and Engineering Tuttlingen (IWAT), Furtwangen University (HFU), Tuttlingen, Germany
[*] Corresponding author, email: mo.li@hs-furtwangen.de

Abstract: The quality and amorphous phase building of metallic glass produced by the selective laser melting (SLM) process can be influenced by the starting powder. In the study, the gas atomised $Ti_{60}Zr_{10}Nb_{15}Si_{15}$ powders were characterised using a range of criteria, including chemical composition, particle size and microstructure. The results suggest that the finer powder in Groups 1 and 2, with a d_{50} of 17.2 and 56.1 µm, respectively, may be more compatible as the starting powder for the production of metallic glass via the SLM process.

I. Introduction

Metallic glass represents a novel class of technical materials that lack crystalline phases and instead exhibit an amorphous microstructure. This microstructure results in enhanced mechanical and chemical properties, including high strength and excellent resistance to wear and corrosion. Such properties render them optimal for utilisation in medical applications, including orthopedic implants. Nevertheless, the component size of metallic glass that can be achieved through conventional techniques, such as casting and melt spinning, remains limited. Selective laser melting (SLM), as one of the additive manufacturing techniques, offers a potential solution by enabling the production of components of a size close to that required for a particular application through the layer-by-layer addition of materials and high cooling rates [1].

In the present study, the $Ti_{60}Zr_{10}Nb_{15}Si_{15}$ powder was evaluated with regard to its suitability as a starting powder for the production of metallic glass by SLM, with a particular focus on its chemical composition, the morphology of the powder, particle size distribution, and microstructure.

II. Material and methods

The powder, with a defined chemical composition of $Ti_{60}Zr_{10}Nb_{15}Si_{15}$ (at.%), was fabricated in three groups by TANIOBIS GmbH through electrode induction melting inert gas atomization (EIGA) under an Argon atmosphere. According to the standard VDI3405, the powder was evaluated based on a series of criteria, including its chemical composition, particle shape, and particle size distribution. The chemical analysis was conducted using an energy-dispersive X-ray fluorescence spectrometer (ED-XRF) in a helium gas atmosphere, while the morphological analysis was performed using scanning electron microscopy (SEM, Zeiss EVO MA 15). The particle size distribution was determined in accordance with the ISO 13322-1 standard using digital light microscopy (Keyence). A phase analysis of the powder was conducted using the Bruker D8 Discover X-ray diffraction (XRD) apparatus with Cu Kα radiation and a scanning rate of 0.04°/s over a 2θ range of 20° to 80°.

III. Results and discussion

The results of the chemical analyses of the powder materials are listed in Table 1. It can be observed that there is a discrepancy between the defined value and the actual silicon (Si) content for all three groups. In addition, the deviation of the zirconium (Zr) content is more significant in Group 3 in comparison to Groups 1 and 2. The observed deviation from the eutectic point, with a composition of 10 at.% Zr and 15 at.% Si, may result in the formation trends of the β-phase in the metallic glass samples produced by SLM with a rapid solidification process.

Table 1 Chemical composition of $Ti_{60}Zr_{10}Nb_{15}Si_{15}$ powder

Group	Ti [at.%]	Zr [at.%]	Nb [at.%]	Si [at.%]
1	Bal.	9.7 ± 0.4	14.8 ± 0.3	13.2 ± 0.9
2	Bal.	9.0 ± 0.1	15.5 ± 0.3	13.6 ± 0.6
3	Bal.	8.7 ± 0.2	15.3 ± 0.6	13.5 ± 0.8

As illustrated in Figure 1 (top), the morphological analysis indicates that the three gas atomised powders exhibit a near-ideal spherical particle morphology. No evidence of powder agglomeration is observed. It is noteworthy that the powder particles in Group 1 exhibit the presence of satellites, which have the potential to influence the flowability of the material. The light microscope images in Figure 1 (middle) demonstrate that the porosity is evident in the cross-

 DOI: 10.5281/zenodo.14269036

sectional view of the polished powders. This is due to the fact that the argon, which was used as a protective gas in the EIGA process, is not fully dissolved in the melt. This can result in the formation of additional pores [2]. This defect has the potential to negatively impact the relative density and mechanical properties of components manufactured using SLM. Nevertheless, the impact of these effects is minimal at low concentrations of pores. As shown in Figure 1 (bottom), the mean particle diameters d_{50} for groups 1 to 3 are 17.2, 56.1 and 71.4 µm, respectively. The fines with a particle size smaller than 17 µm are discernible in groups 1 and 3, as they cannot be completely removed by sieving processes. The particle size distribution exerts a significant influence on the flowability and spreadability of the powder, as well as its laser absorption capacity in the context of additive manufacturing. Moreover, the thermal conductivity of a powder bed can be altered by particle size [3]. The microstructure of SLM manufactured metallic glasses is influenced by the alteration in laser absorptivity and thermal conductivity caused by different particle sizes due to the very high sensitivity of the thermal history. Therefore, the finer particle sizes in Groups 1 and 2 can improve the manufacturability of the amorphous phases of metallic glass in the SLM process.

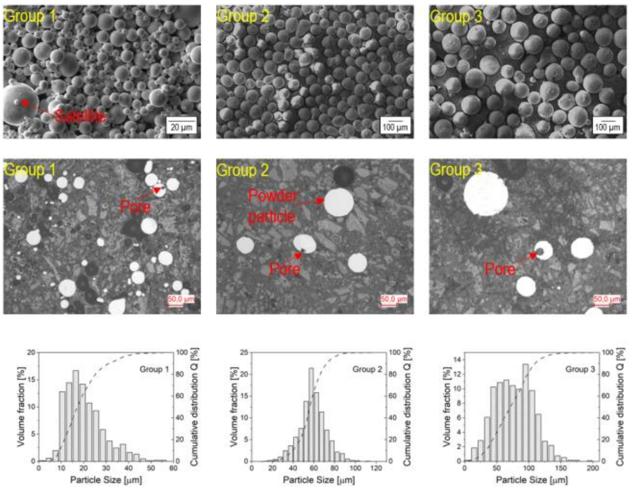

Figure 1 The morphology of the gas atomised powder analysed using a scanning electron microscope (SEM) (top); the polished powder analysed using a light microscope (middle); and the particle size distribution of the three groups of powder (bottom)

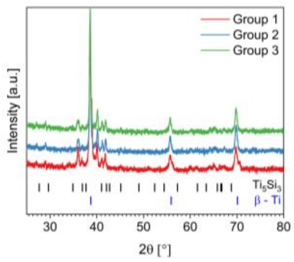

Figure 2 XRD patterns of $Ti_{60}Zr_{10}Nb_{15}Si_{15}$ powders

The XRD results of the powder materials depicted in Figure 2 demonstrate the presence of crystalline peaks associated with the β-Ti and Ti_5Si_3 phases, with no evidence of a typical broad, flat peak indicative of an amorphous structure across all three groups. Figure 3 shows the microstructure of powders, which comprises two types of crystals: dark-coloured polyhedral Ti_5Si_3 and light-coloured β-Ti with a globular grain structure. Moreover, the unmelted Niobium (Nb) within the core of the particle in Group 3 is clearly seen, as Nb, due to its high melting temperature of 2750 °C, is not fully melted during the EIGA process and remains within the powder. It seems unlikely that such unmelted Nb particles will be present in the starting powder, as they are also usually difficult to melt during the SLM process [4]. Consequently, these Nb particles in Group 3 may persist as foreign nuclei during solidification, potentially influencing the formation of a high amorphous phase fraction.

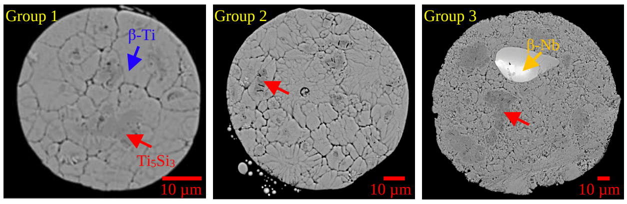

Figure 3 Scanning electron micrograph (BSE) of the etched powders for phase analysis

IV. Conclusions

The characterisation of the three group gas atomised powders reveals a slight deviation of Si from the defined chemical component, which is particularly evident in Group 3 for Zr. This may result in the formation of the β-phase by the SLM process. The analysis of morphology shows that all groups exhibit a near-ideal spherical powder form, which is advantageous for flowability and spreadability in the SLM process. Moreover, the powders in Groups 1 and 2 display a more refined particle size distribution, with d_{50} values of 17.2 and 56.1 µm, respectively. Additionally, the powders contain two crystalline phases: β-Ti and Ti_5Si_3. In contrast, the powder in Group 3, which has a larger particle size, contains unmelted Nb, which has a negative effect on the formation of the amorphous phase by SLM. It can therefore be concluded that the powder in Groups 1 and 2 may be more suitable as a starting powder for the production of metallic glass via the SLM process.

Acknowledgments

The authors would like to express their gratitude to the BMBF and the industry partners, namely TANIOBIS GmbH and B. Braun in Germany (Aesculap AG), for their financial support.

Author's statement

Research funding: This research has been funded by the German Federal Ministry of Education and Research (BMBF) under grant agreement no. 13FH5I07IA (CoHMed / SmartMed-A). Conflict of interest: Authors state no conflict of interest. Informed consent: Informed consent has been obtained from all individuals included in this study. Ethical approval: The research related to human use complies with all the relevant national regulations, institutional policies and was performed in accordance with the tenets of the Helsinki Declaration, and has been approved by the authors' institutional review board or equivalent committee.

References

[1] W. Wu, et. al., *Additive manufacturing of bulk metallic glass: Principles, materials and prospects,* Materials Today Advances, vol. 16, Dec. 2022.

[2] S. Luo, et. al., *Interaction between high-velocity gas and liquid in gas atomization revealed by a new coupled simulation model,* Materials & Design, vol. 212, 2021.

[3] Q.B. Nguzen, et. al., *Characteristics of Inconel Powders for Powder-Bed Additive Manufacturing,* Engineering, vol. 3, pp. 695–700, 2017.

[4] I. Polozov, et. al., *Synthesis of Ti-5Al, Ti-6Al-7Nb, and Ti-22Al-25Nb alloys from elemental powders using powder-bed fusion additive manufacturing,* Journal of Alloys and Compounds, vol.763, pp. 436–445, 2018.